Neural control of hepatic lipid metabolism: A (patho)physiological perspective

Bruinstroop, E.

Publication date
2013

2

SPINAL PROJECTIONS OF THE A5, A6 (*LOCUS COERULEUS*), AND A7 NORADRENERGIC CELL GROUPS IN RATS

Eveline Bruinstroop, Georgina Cano,
Veronique G.J.M. VanderHorst, Judney C. Cavalcante,
Jena Wirth, Miguel Sena-Esteves and Clifford B. Saper

Journal of Comparative Neurology 2012; 520:1985-2001

ABSTRACT

The pontine noradrenergic cell groups, A5, A6 (*locus coeruleus*), and A7, provide the only noradrenergic innervation of the spinal cord, but the individual contribution of each of these populations to the regional innervation of the spinal cord remains controversial. We have used an adeno-associated viral (AAV) vector encoding green fluorescent protein under an artificial dopamine beta-hydroxylase (PRSx8) promoter, to trace the spinal projections from the A5, A6, and A7 groups. Projections from all three groups travel through the spinal cord in both the lateral and ventral funiculi and in the dorsal surface of the dorsal horn, but A6 axons take predominantly the dorsal and ventral routes, whereas A5 axons take mainly a lateral and A7 axons a ventral route. The A6 group provides the densest innervation at all levels, and includes all parts of the spinal gray matter, but it is particularly dense in the dorsal horn. The A7 group provides the next most dense innervation, again including all parts of the spinal cord, but is it denser in the ventral horn. The A5 group supplies only sparse innervation to the dorsal and ventral horns and to the cervical and lumbosacral levels, but provides the densest innervation to the thoracic intermediolateral cell column, and in particular to the sympathetic preganglionic neurons. Thus, the pontine noradrenergic cell groups project in a roughly topographic and complementary fashion onto the spinal cord. The pattern of spinal projections observed suggests that the *locus coeruleus* might have the greatest effect on somatosensory transmission, the A7 group on motor function, and the A5 group on sympathetic function.

INTRODUCTION

Noradrenergic axons are found throughout the spinal cord, but are most concentrated in the superficial dorsal horn, the ventral horn motoneuron pools, lamina X, and the thoracic and sacral intermediolateral cell columns (IML) (1,2). Early studies, using retrograde transport of horseradish peroxidase combined with immunostaining for dopamine beta-hydroxylase (DBH) or retrograde transport of anti-DBH antibodies, demonstrated that the noradrenergic innervation of the spinal cord arises from the A5, A6 (*locus coeruleus*; LC) and A7 cell groups in the pons (1-3). However, previous attempts to determine which parts of the spinal projection arise from which noradrenergic neurons have produced conflicting results.

Fritschy, Grzanna and colleagues (2,4) used the combination of anterograde transport of *Phaseolus vulgaris* lectin (PHA-L) with immunohistochemistry for DBH in Sprague-Dawley rats to demonstrate that LC axons run predominantly through the superficial layers of the dorsal horn to innervate mainly dorsal horn targets. After injections of a retrograde tracer into the cervical spinal cord they found more retrogradely labeled neurons in the LC, whereas more retrogradely labeled neurons were present in A5 following thoracic injections, and more A7 neurons labeled from lumbar injections. The projections from all three groups were bilateral, with a slight ipsilateral predominance. They subsequently treated the rats with the noradrenergic neurotoxin N-(2-chloro-ethyl)-N-ethyl-2-bromobenzylamine (DSP-4) intraperitonally, which selectively damages axon terminals originating in the LC (5). In these rats DBH immunohistochemical staining was abolished in the dorsal horn and intermediate zone, whereas noradrenergic terminals were still visible in the ventral horn and IML (2).

By contrast, Clark and Proudfit (6), using very similar methods also in Sprague-Dawley rats, reported that LC axons projected predominantly through the ventral funiculus and innervated mainly the ventral horn and central gray area of the spinal cord. Lesions of the LC caused slightly lower numbers of DBH-immunoreactive (DBH-ir) axons in the ipsilateral than the contralateral ventral horn in all five cases studied, but there were reductions in the ipsilateral dorsal horn in two cases as well. Because of the disparity in their results compared to those of Fritschy and Grzanna, Clark *et al*. (7) examined retrograde transport of Fluorogold from the ventral or dorsal horn in Sprague-Dawley rats obtained from Harlan, which Fritschy and Grzanna had used, and in rats obtained from Sasco, the supplier in their own previous study. They found that there were more retrogradely labeled neurons in the LC from the spinal ventral horn injections in the rats from Sasco, and concluded that the disparities in the results were due to the difference in the substrain sold by the different vendors. However, this experiment involved only two rats per group (four from each vendor, two dorsal and two ventral horn injections), all injections were made at a lumbar level (which according to Fritschy and Grzanna has the least LC innervation), and some of the ventral horn injections clearly invaded the dorsal horn.

One limitation with the methods used in these studies is that there are non-noradrenergic neurons near the LC (in Barrington's nucleus), the A7 group (in the Kölliker-Fuse nucleus), and the A5 group (in the ventrolateral pontine reticular formation dorsal to A5) that also project to the spinal cord. Thus, when a non-selective anterograde transport marker like

PHA-L is used, it must be combined with immunostaining for DBH to identify noradrenergic axons. Double axonal staining must be demonstrated using fluorescence, and this method may not be sensitive enough to identify all of the DBH-containing axons. Thus, it is not clear that either study gauged the entire extent of the descending noradrenergic axons from the A5 vs. the A6 vs. the A7 groups.

We sought to obtain a more accurate perspective on the noradrenergic projections to the spinal cord by using a genetically-specified viral vector-based tracing method. We generated an adeno-associated viral (AAV) vector encoding green fluorescent protein (GFP) driven by the PRSx8 promoter. This is sometimes described as a synthetic DBH promoter (Hwang *et al.*, 2001), and consists of eight copies of a promoter sequence from the *cis*-regulatory region of the DBH gene that binds the phox2a/b transcription factors. This promoter sequence is thought to drive gene expression at a high level specifically in neurons expressing the phox2a/b transcription factors, which are critical for the catecholaminergic phenotype (8-10). As the A5, A6 and A7 cell groups co-express DBH and Phox2, but the other spinally projecting cell groups adjacent to them do not (11), injection of the AAV with the PRSx8 promotor should selectively drive GFP expression in the noradrenergic-spinal cell groups. This promoter sequence has been used previously for anterograde and retrograde tracing of catecholaminergic neurons (12,13), although there is evidence that some non-catecholaminergic neurons may also be labeled. Hence, we employed this method, with additional controls to insure that we could identify the projections of the A5, A6 and A7 cell groups, without the confound of labeling from other cell groups, at different levels of the spinal cord.

MATERIALS AND METHODS

Animals

Adult male Sprague Dawley rats (n = 18; weight 275-325 g) from Harlan were housed individually under a 12 h light/dark cycle (lights on at 7:00 A.M.) at 22°C, with *ad libitum* access to food and water. All procedures conformed to the regulations detailed in the National Institutes of Health *Guide for the Care and Use of Laboratory Animals* and were approved by the Institutional Animal Care and Use Committee of Harvard Medical School.

Viral vector

The AAV vector carrying the PRSx8 promoter (14) was prepared by using PCR amplification of a plasmid containing PRSx8 kindly provided by Dr. Kwang-Soo Kim using the following primers (restriction sites underlined): sDBH-1 AATTGGTACCACGACGGCCAGTGCCTAGCTTCCGCTA; sDBH-2: TTTTAAGCTTGTCGGCTGGGGTGAGCTCACTGG. The resulting PCR product was digested with Eco RI and Hind III and used to replace the CBA promoter in the pAAV-CBA-EGFP-W plasmid (15) digested with the same enzymes to generate the plasmid pAAV-PRSx8-EGFP-W. The AAV2/rh8-PRSx8-EGFP-W vector stock was produced, purified, and titer determined as previously described (15). The titer of the vector stock was 8×10^{13} genome copies (gc)/mL. After delivery to the brain, this AAV vector will only express GFP in cells containing the phox2a/b transcription factors which bind to the PRSx8 promoter.

Surgery

Rats were anesthetized with chloral hydrate (350 mg/kg i.p.). The skull was exposed and a hole was drilled. Unilateral microinjections of the AAV vector (65-100 nl) were placed stereotaxically into the LC (n = 6), A7 (n = 6), or A5 (n = 6) cell groups using a glass micropipette and an air pressure-driven delivery system. The coordinates for the LC were: AP -9.6, DV -5.9, RL -1.05; for A7: AP -8.7, DV -6.7, RL -2.2; and for A5: AP -9.2, DV -8.3, RL -2.5. The skin was closed with wound clips, and the rats were treated with the analgesic Flunixin for 48 hours postoperatively.

Perfusion

A survival time of 4 weeks was chosen between injection of the tracer and perfusion based on earlier studies from our laboratory (16). After 4 weeks the rats were deeply anesthetized with chloral hydrate (500 mg/kg) and perfused transcardially with 100 ml of saline followed by 400 ml of 10% neutral phosphate-buffered formalin. Brains and spinal cords were removed and postfixed for 3 h in formalin and then transferred to 20% sucrose overnight.

Immunohistochemistry

Brains were sectioned on a freezing microtome at 35 µm into five series. Spinal cords were blocked for longitudinal sections (C1-7, T2-7, T10-L1, L4-S4) and transverse sections (C8-T1, T8-9, L2-3), and were sectioned at 40 µm into one series for the longitudinal sections and five series for the transverse sections. To detect GFP signal, an immunoperoxidase staining procedure was performed in a set of spinal cord and brain sections. First, sections were washed several times in 0.1 M phosphate buffered saline (PBS), pH 7.4, for 1 h, then incubated in 0.3% hydrogen peroxide in PBS containing 0.3% Triton X-100 (PBT) to remove endogenous peroxidase activity, and washed again in PBS for 30 min. Sections were incubated in the primary antiserum anti-GFP (1: 10,000) in PBT overnight at room temperature. Sections were rinsed in PBS and incubated in biotinylated anti-rabbit antibody (1:1,000, Jackson ImmunoResearch) in PBT for 1 h, rinsed three times in PBS, and incubated in avidin–biotin complex (Elite ABC, Vector Laboratories) for 1 h. After three rinses, sections were incubated in 1% diaminobenzidine (DAB), 0.05% nickel ammonium sulfate, and 0.05% cobalt chloride, and reacted with 0.01% hydrogen peroxide to obtain a black precipitate for GFP detection. Sections were washed, mounted on gelatin-coated glass slides, dehydrated in graded alcohols, cleared in xylene, and coverslipped.

To examine the neuroanatomical relation between noradrenergic projections and spinal cholinergic neurons (mainly sympathetic preganglionic neurons and somatic motoneurons), one set of spinal cord sections was double stained first for GFP (following the protocol detailed above) and then incubated in anti-choline acetyltransferase (ChAT) antibody, which labels cholinergic neurons. Briefly, sections were incubated overnight at room temperature in goat anti-ChAT (1: 500) in PBT, rinsed in PBS and incubated in biotinylated anti-goat antibody (1:1,000, Jackson ImmunoResearch) in PBT for 1 h, rinsed in PBS, incubated in avidin–biotin complex for 1 h, and finally incubated in 1% DAB and reacted with 0.01% hydrogen peroxide to obtain a brown precipitate. Following this dual staining procedure, spinal cholinergic neurons were identified by their brown cytoplasm whereas GFP (noradrenergic) projections were labeled in black.

To enhance GFP labeling for better visualization, one set of spinal coronal sections and one set of longitudinal sections were stained following the immunoperoxidase method with DAB described above (without 0.05% nickel ammonium sulfate and 0.05% cobalt chloride in the final incubation step) and further processed for silver enhancement. After DAB staining, the sections were mounted on gelatin-coated glass slides. The slides were incubated in 1% silver nitrate solution at 56°C for 30-45 minutes, after which the sections were rinsed with water and changed to 0.1% gold chloride solution for 10 minutes. The sections were rinsed and changed to 5% sodium thiosulfate. Finally the sections were washed and dehydrated in a series of graded ethanols and then cleared in xylene. Another set of spinal cord sections was used for dual-fluorescence labeling of GFP and ChAT. Sections were washed in 10mM PBS, and blocked with 3% donkey serum. The sections were incubated in the primary antisera containing rabbit anti-GFP (1:15,000) and goat anti-ChAT (1:500) overnight. The sections were washed several times and incubated in a mix of secondary fluorescent antibodies in PBT: Alexa Fluor 555-conjugated donkey anti-goat IgG and Alexa Fluor 488-conjugated donkey anti-rabbit IgG (both at 1:500; Invitrogen) for 2 hours at room temperature. The sections were washed several times, mounted on gelatin coated slides, dehydrated in graded alcohols, cleared in xylenes for 1 minute and coverslipped.

To determine whether all GFP immunoreactive (GFP-ir) structures (cell bodies and projections) were noradrenergic, dual immunofluorescence labeling for GFP and DBH was performed in one set of spinal cord sections and one set of brain sections, as described above. The sections were incubated in the primary antisera containing rabbit anti-GFP (1:3,000) and mouse anti-dopamine β-hydroxylase (1:3,000) overnight. Alexa Fluor 488 donkey anti-rabbit IgG (1: 500; Invitrogen A21206, lot#: 439378) was used to label GFP in green and Alexa Fluor 555 donkey anti-mouse IgG (1:500; Invitrogen A31570, lot#: 412442) to label DBH in red.

To determine whether all labeled cells in the injection site were neurons, another set of brain sections was stained for dual-fluorescence for GFP and NeuN, a standard neuronal marker. Sections were incubated in mouse anti-NeuN (1:20,000) and rabbit anti-GFP (1:15,000) overnight. A similar protocol as described above was used with the secondary antibodies Cy3-conjugated Affinipure donkey anti-mouse and Cy2-conjugated Affinipure donkey anti-rabbit IgG (both at 1:500; Jackson ImmunoResearch) to produce dual immunofluorescence images (GFP in green and Neu-N in red). The sections were washed several times, and mounted, dehydrated, cleared, and coverslipped as explained above.

Characterization of primary antibodies

All antibodies used and their immunogens are identified in Table 1.

To detect GFP, an anti-GFP rabbit antibody was used. The anti-GFP did not produce any labeling in brains from rats that had not received injections of the AAV vector containing the GFP gene.

The mouse anti-dopamine β-hydroxylase was used for the detection of noradrenergic neurons. This antibody stains a band of 70 kDa corresponding to DBH and a 140kDa band presumably corresponding to a dimer, in horse ileal tissue (17), and staining in rat brain is abolished by preadsorption with a 10-fold excess of bovine adrenal DBH protein (18).

Table 1. Characteristics of Primary Antibodies.

Antibody	Immunogen	Manufacturer, cat. no., species, type
GFP	GFP isolated from *Aequorea victoria*	Invitrogen; A6455 #57204A; rabbit polyclonal
DBH	Purified bovine adrenal DBH	Millipore; MAB308 #23090206; mouse monoclonal, clone 4F10.2
ChAT	Human placental enzyme	Millipore; AB144P # 0509011823; goat polyclonal
NeuN	Purified cell nuclei mouse brain	Millipore; MAB377; mouse monoclonal

The cellular morphology and distribution of labeling in the rat pons with this antibody was essentially identical to that observed in previous studies (6,19,20)

The affinity-purified goat anti-ChAT antibody produces a 68-70 kDa band in immunoblotting assays of rat brain and stains a pattern of cellular morphology and a distribution of staining of neurons in the rat spinal cord identical to previous reports (21).

The mouse anti-NeuN antibody recognizes two or three bands in the 46-48 kDa range and possibly another band at approximately 66 kDa in Western blots of rat brain (manufacturer's data sheet). It also stains neurons in brain tissue sections in a pattern that was identical to that in previous descriptions (22).

Illustrations

The spinal cord sections with immunoperoxidase staining for GFP were analyzed at four different levels (C7-8, T1-2, T8-9, L3-4). Using a camera lucida attachment on a Zeiss AxioSkop microscope (Carl Zeiss B.V., Sliedrecht, NL), labeled axons in the spinal cord sections were drawn at high magnification (20X). For both the LC and A7 injection cases, one section was used for each illustration. Because of the sparse spinal innervation found in A5 injection cases, axons observed in 3 consecutive sections were superimposed into one illustration. The drawings were scanned and imported into Adobe Illustrator where they were traced and labeled. Illustrations of the injection sites were also drawn using camera lucida, with each dot representing a GFP-ir cell.

Photomicrographs

The injection sites were analyzed using dual labeling immunofluorescence for GFP in combination with DBH or NeuN. These images were captured with a Zeiss Axioplan 2 microscope with a 1.5 megapixel black/white Evolution QEi camera (MediaCybernetics, Bethesda, MD, USA). Zeiss filterblocks 10 and 20 were used. The immunoperoxidase images of the injection sites and spinal cord sections were captured with a Zeiss Axioplan 2 microscope with 5 megapixel color Evolution MP camera (MediaCybernetics, Bethesda, MD, USA). In Figure 7, the density of the brown DAB staining was de-emphasized with selective color adjustment in Photoshop, to allow clearer distinction from the black staining of labeled axons.

The dual labeling immunofluorescence images of the spinal cord were taken on a Zeiss LSM 510 meta confocal microscope with an Argon 488 laser (BP filter 500-530) and 543 laser (LP filter). Images were saved as z-stacks of 1 µm planes. The z-stacks were processed either

in Image Pro Plus version 6.3 (MediaCybernetics, Bethesda, MD, USA) or in ImageJ (NIH), in which the images in each channel were despeckled and projections prepared of the maximal density at each point, and then the two channels were merged. Individual 1 µm planes were viewed as merged channels. All photomicrographs were then opened in Adobe Photoshop and the contrast and brightness of the red and green channels were adjusted individually to balance the density.

RESULTS

Injection sites

We used an AAV vector carrying the synthetic PRSx8 promoter in an attempt to restrict GFP expression, which fills neuronal bodies and processes, to catecholaminergic neurons targeted

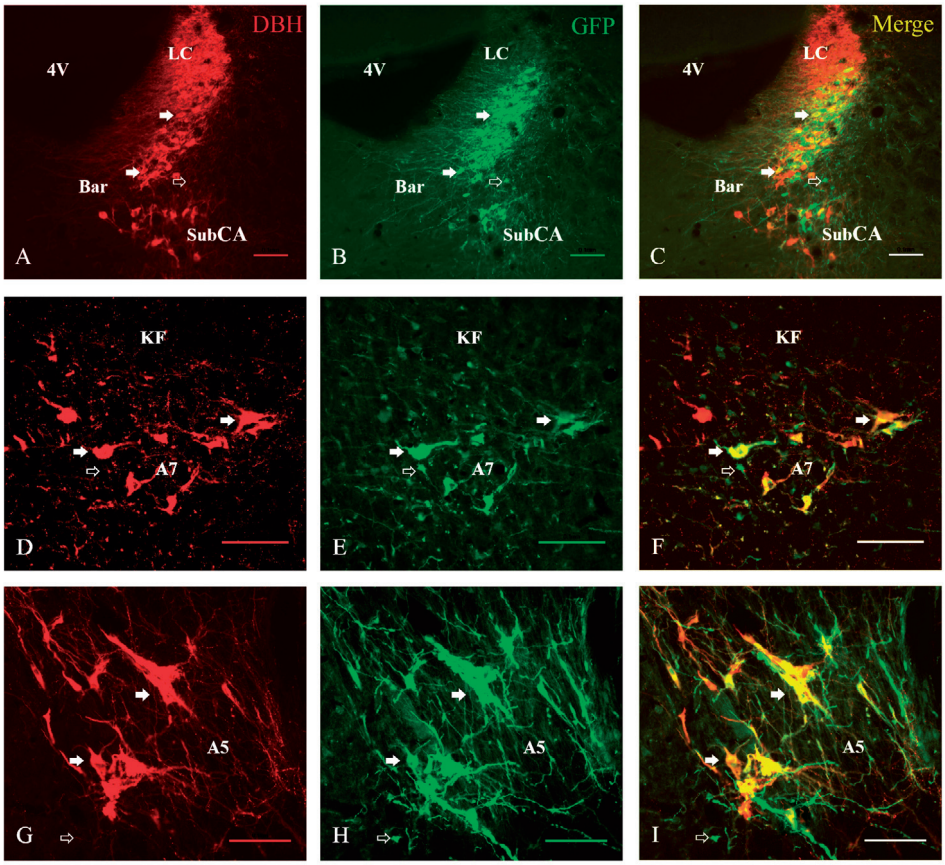

Figure 1. Double labeling of injection sites for DBH immunoreactivity (magenta; A,D,G) and GFP-labeling (green; B,E,H) and merged images (showing doubly labeled neurons in white) after injections into the LC (A-C), A7 (D-F) and A5 (G-I) cell groups. While most of the GFP-labeled neurons were also immunoreactive for DBH (closed arrows), a few small GFP-labeled cells were seen (open arrows) that were not DBH-immunoreactive. Scale bars: 0.1 mm.

by stereotaxic injection. From the 18 rats injected (LC n = 6, A7 n = 6, A5 n = 6) with the viral vector, 8 cases (LC n = 2, A7 n = 3, A5 n = 3) were selected for detailed analysis based upon the presence of substantial double labeling for GFP and DBH (Figure 1), indicating that these injections involved the respective noradrenergic cell groups. Small, round GFP-ir cells which were not DBH-ir were observed at the center of each injection site. All of these cells were double labeled for GFP and the neuronal-specific marker NeuN, indicating that they were neurons. Nevertheless, in these cases, none of these non-DBH cells were located within cell groups known to project to the spinal cord such as Barrington's nucleus, the Kölliker-Fuse nucleus, or the reticular formation dorsal to the A5 cell group. In addition, double label experiments using confocal microscopy determined that essentially all of the GFP-labeled axons in the spinal cord also stained for DBH (Figure 2). Hence, we are confident that the spinal projections in these cases represent efferents only from noradrenergic neurons. All GFP-ir neurons at the injection sites of one representative case from the A5, A6, and A7 groups are shown in Figure 3.

Spinal projections

The projections at different levels of the spinal cord were compared among cases from each injection group (LC, A7 and A5), and these projections showed the same pattern across cases with similarly located injection sites. GFP-ir fibers at four levels of the spinal cord (C7-8, T1-2, T8-9, L3-4) from a representative case from LC, A7 and A5 injections, respectively, are shown in Figure 4. The sacral spinal cords were all cut in the horizontal plane (see Methods), but the pattern of labeling was very similar to that of the lumbar cord, with the exception of the IML, as noted below.

Spinal projections from the locus coeruleus (A6)

Following injections into the LC, GFP-ir descending axons in the spinal white matter were most numerous in the ipsilateral ventral funiculus and the superficial dorsal horn (Figure 5A). However, labeled axons were also plentiful in the ipsilateral and contralateral lateral funiculus. A few axons were also found in the ipsilateral dorsal funiculus and contralateral ventral funiculus (Figure 4).

Anterogradely labeled axons were found to ramify in all layers of the spinal cord, but were most dense in the dorsal horn particularly along its superficial margin with Lissauer's tract (Figures 4 and 6A). Nevertheless, there was substantial axonal labeling in the deeper layers of the dorsal horn, the intermediate layers, around the central canal, and in the ventral horn. The density and relatively random pattern of labeled axons in the lateral cervical nucleus was not different from the deep layers of the dorsal horn. There was no apparent concentration of axons in any particular structures within these spinal laminae (such as the phrenic motor nucleus or the IML in the thoracic or sacral spinal cord), but neither did the axons avoid these regions. The densities of labeled axons in each spinal lamina were similar at all spinal levels in each case, although there was a slight tendency for LC axons to be more prominent in the cervical and lumbar enlargements (which are concerned with sensation and movement in the distal limbs). Compared to the axon trunks in the descending tracts, which tended to be relatively thick and straight and not to have boutons along their length (Figure 5A), axonal ramifications in the gray matter were thinner, took a more meandering course, tended to give off multiple branches, and were studded with varicosities along their lengths (Figures 7B, C).

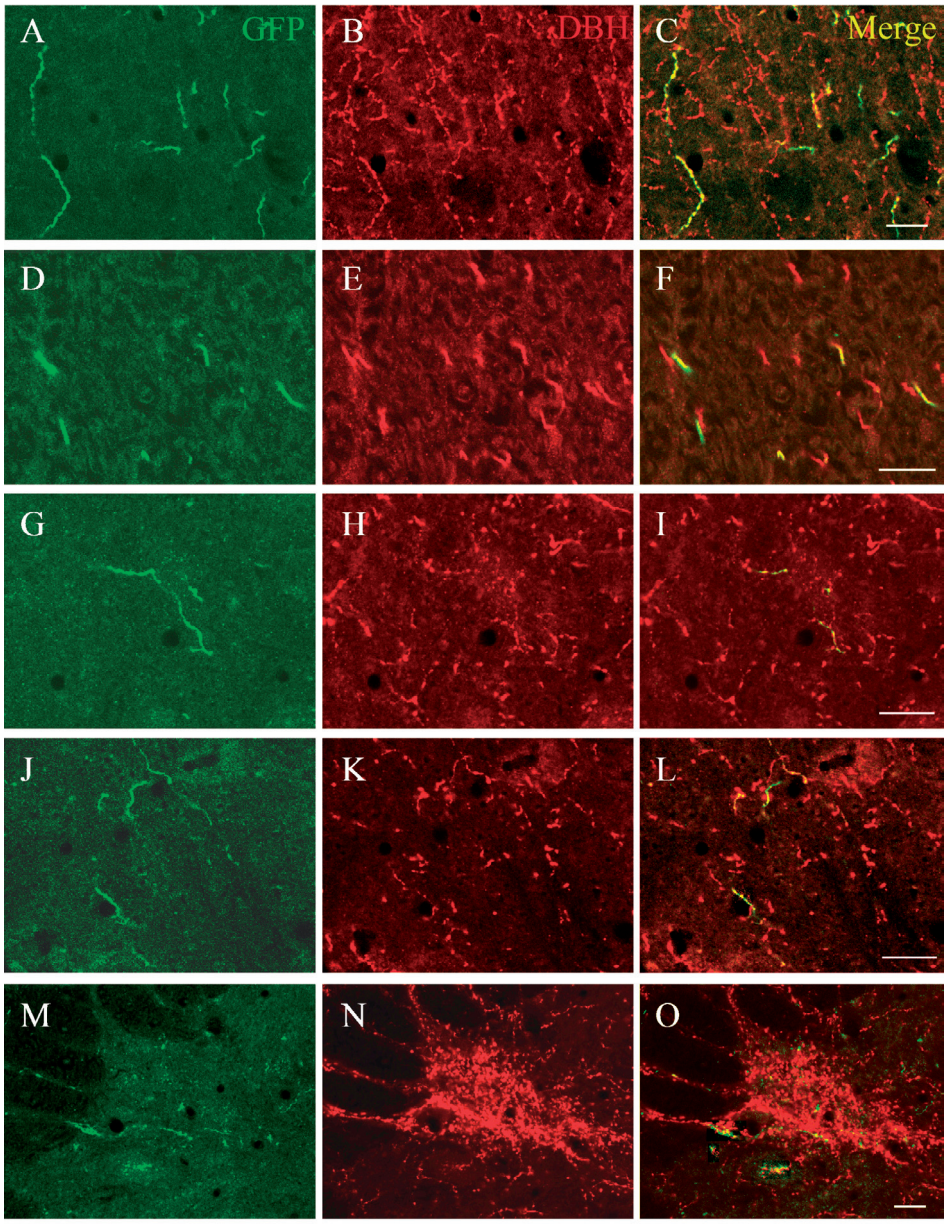

Figure 2. A series of immunofluorescence photomicrographs showing that GFP-labeled axons in the spinal cord were also DBH-immunoreactive. GFP-immunoreactive axons are shown in green (A, D,G,J,M), DBH-labeled axons in magenta (B,E,H,K,N), and overlap in white (C,F,I,L,O). Images show staining of axons from LC running through the dorsal horn (A-C), and ventral funiculus (D-F), from A7 in the ventral horn (G-I; J-L), and from A5 in the IML (M-O). Note that GFP staining fills the axons, but that DBH immunoreactivity is predominantly associated with varicosities in thin, ramifying axons. Scale bar for all images: 0.02 mm.

Figure 3. A series of drawings to illustrate the distribution of labeled neurons in the injection sites in the A7 (left), LC (center) and A5 (right) groups in three representative animals. Every dot represents a single GFP-ir cell stained with the immunoperoxidase method in one representative case for each injection site.

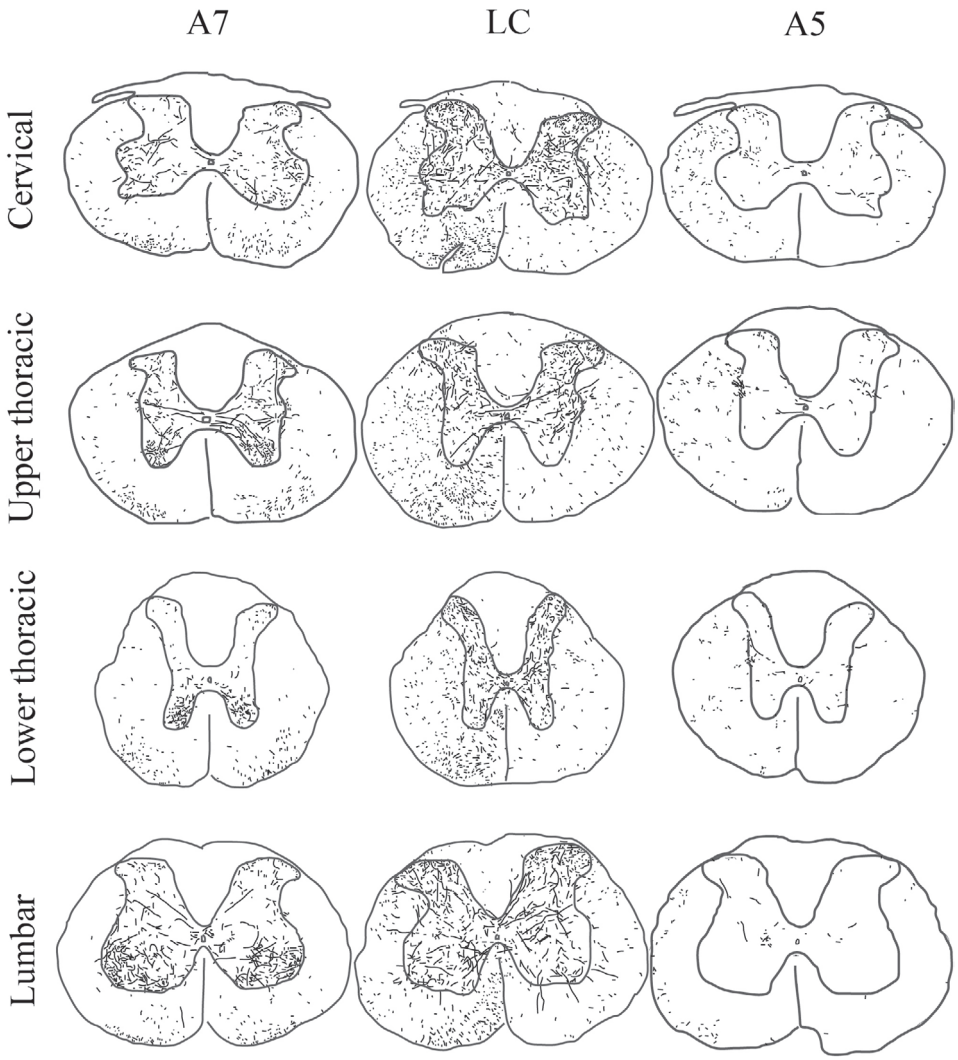

Figure 4. Drawings of labeled axons in the spinal cord of one representative case from A7 (left), LC (center) and A5 (right) injections, respectively. The spinal cord is shown at Cervical (C7-8), Upper thoracic (T1-2), Lower thoracic (T8-9) and Lumbar (L3-4) levels. For the LC and A7 cases, axons observed in one single section are shown. Because of the sparse spinal innervation found in A5 injection cases, axons observed in 3 consecutive sections were superimposed into one illustration.

Spinal projections from A7

After injections into the A7 cell group, GFP-ir descending axons in the white matter were found mainly in the ventral funiculus bilaterally. Smaller numbers of labeled axons were observed in the lateral funiculus, with an ipsilateral predominance. In the gray matter, as with the LC axons, those from the A7 cell group ramified extensively, giving off varicose branches that wove along the dendrites and cell bodies of motoneuron groups in the

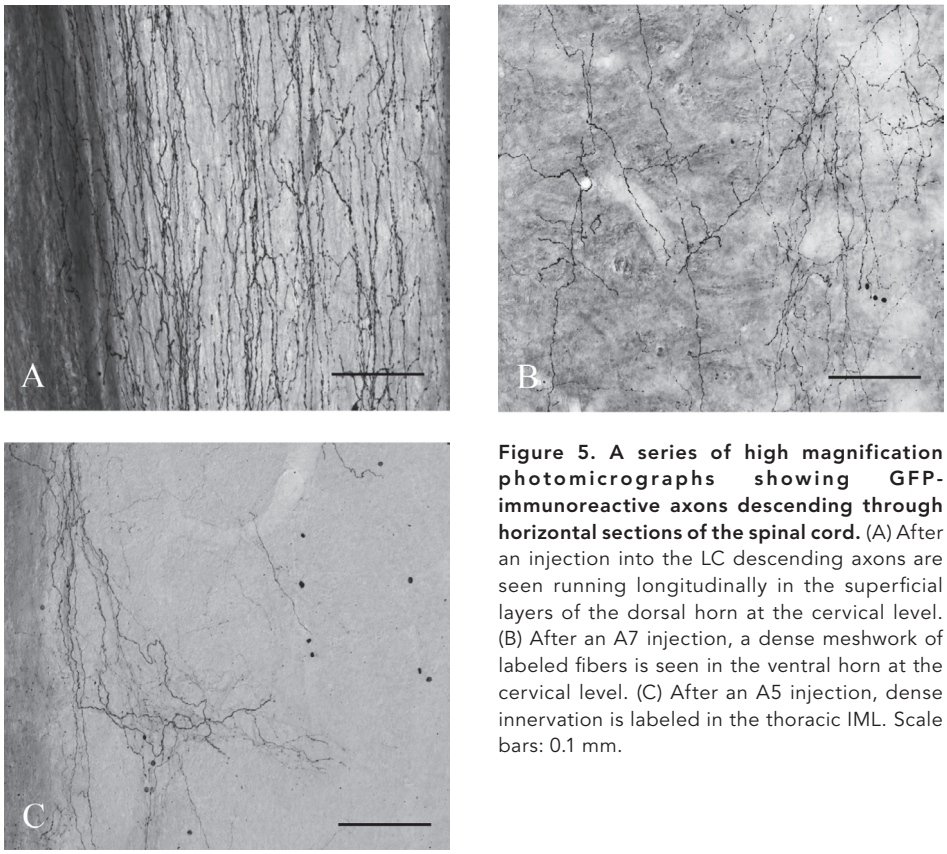

Figure 5. A series of high magnification photomicrographs showing GFP-immunoreactive axons descending through horizontal sections of the spinal cord. (A) After an injection into the LC descending axons are seen running longitudinally in the superficial layers of the dorsal horn at the cervical level. (B) After an A7 injection, a dense meshwork of labeled fibers is seen in the ventral horn at the cervical level. (C) After an A5 injection, dense innervation is labeled in the thoracic IML. Scale bars: 0.1 mm.

ventral horn (Figures 4, 5B, 6B, 8F,I, 9E-H). Smaller numbers of labeled axons were found in the dorsal horn, particularly its superficial layers, and in the IML at thoracic levels (Figure 7C).

A7 axons were found most densely in the lumbar spinal cord. However, at this level there were no labeled axons in the lateral funiculus.

Spinal projections from A5

Following injections into the A5 cell group, a much smaller contingent of GFP-ir axons was observed. Most descending axons were found in the ipsilateral lateral funiculus, but smaller numbers of labeled axons were also seen in the ventral funiculus and on the contralateral side. A5 axons within the spinal gray matter ramified extensively and gave off profuse boutons bilaterally in the thoracic IML, but substantial numbers of varicose axons were also seen in the dorsal commissural region, and the intermediate gray matter connecting these two regions, which are the areas containing the majority of sympathetic preganglionic neurons (23) (Figures 4, 5C, 6C, 7J-L). In addition, smaller numbers of labeled axons were seen in the dorsal and ventral horns at all levels. At sacral levels, the A5 axons also ramified

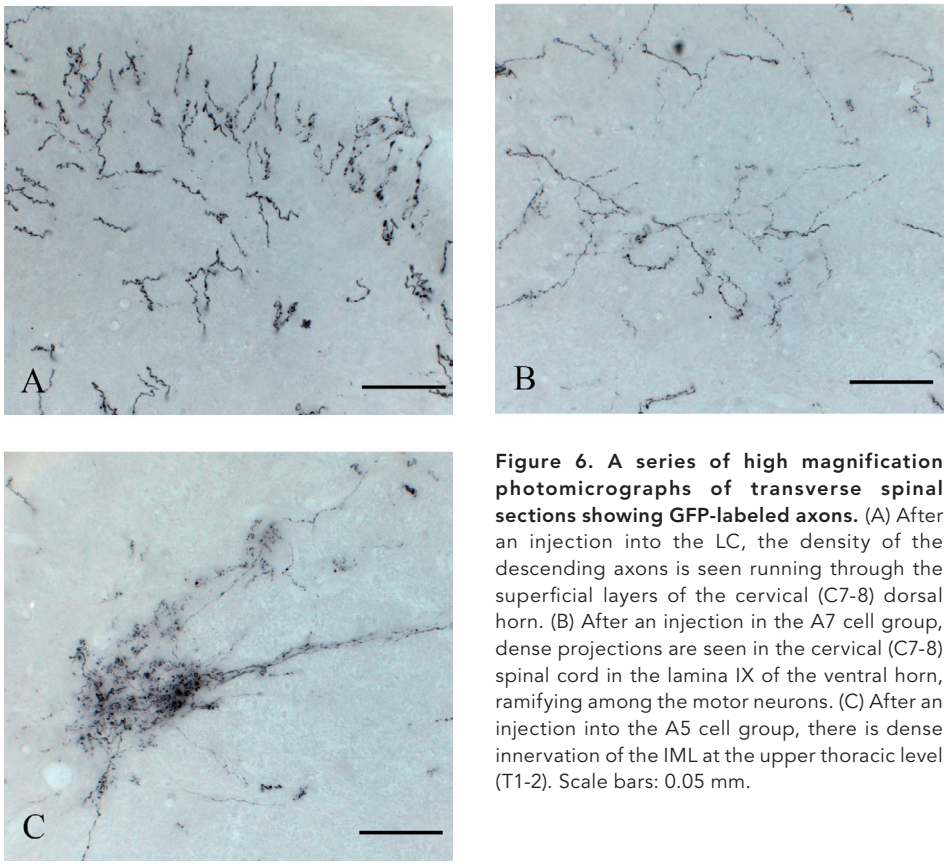

Figure 6. A series of high magnification photomicrographs of transverse spinal sections showing GFP-labeled axons. (A) After an injection into the LC, the density of the descending axons is seen running through the superficial layers of the cervical (C7-8) dorsal horn. (B) After an injection in the A7 cell group, dense projections are seen in the cervical (C7-8) spinal cord in the lamina IX of the ventral horn, ramifying among the motor neurons. (C) After an injection into the A5 cell group, there is dense innervation of the IML at the upper thoracic level (T1-2). Scale bars: 0.05 mm.

more profusely in the intermediate gray matter and the IML than in the dorsal or ventral horns, but the density of IML innervation was not nearly as striking as at thoracic levels.

The densest innervation was observed at the upper thoracic level of the spinal cord. Labeled axons in the ventral funiculus were most dense at the lower cervical level and the density decreased in consecutive caudal levels.

Relationship of noradrenergic descending axons with cholinergic neurons in the spinal cord

For each case, a set of spinal cord sections was doubly labeled for GFP and ChAT for light microscopy (Figure 7) and a second series for confocal microscopy (Figures 8,9) to examine the anatomical relationship of the descending noradrenergic innervation to the cholinergic neurons of the spinal cord (mainly autonomic preganglionic neurons and somatic motoneurons). Unfortunately, because the sacral spinal cords had been cut in the horizontal plane, no sections were available from that level for this double staining.

After injections into the LC, there were profuse labeled axons in the dorsal horn, particularly along its superficial margin with Lissauer's tract (Figure 7A), and numerous labeled axons were also observed throughout the dorsal horn, especially at its base

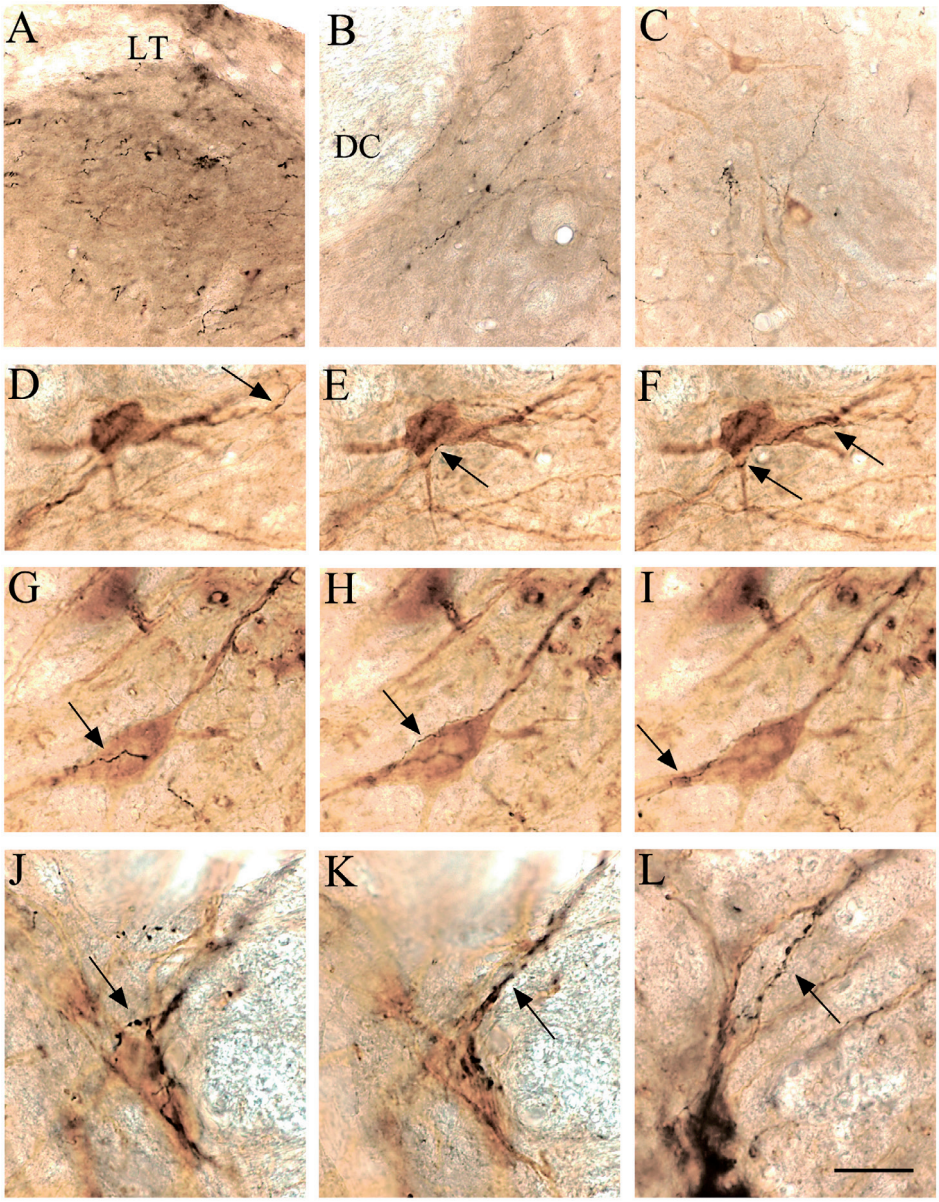

Figure 7. Photomicrographs showing the relationship of the GFP-ir fibers (black) to cholinergic neurons (brown staining for ChAT) in the spinal cord. LC axons in the dorsal horn were observed along its superficial margin with the Lissauer's tract (LT) (panel A), and were numerous throughout the dorsal horn, especially at its base adjacent to the dorsal columns (DC) (panel B). In the ventral horn, labeled axons were not located adjacent to cholinergic neurons (C). In contrast, anterogradely labeled axons from A7 neurons ran along the surface of the cell bodies and proximal dendrites of ventral horn cholinergic neurons, as shown in two series of photomicrographs taken at 3 different focal planes through a pair of cholinergic neurons (D-F and G-I), respectively. Following A5 injection, labeled axons showed intense ramification and numerous boutons along the cell bodies and proximal dendrites of cholinergic neurons in the IML at the thoracic level (J and K are two focal planes through the same neurons, L is a different field). Scale bar: 50 μm for A-C; 25 μm for D-L.

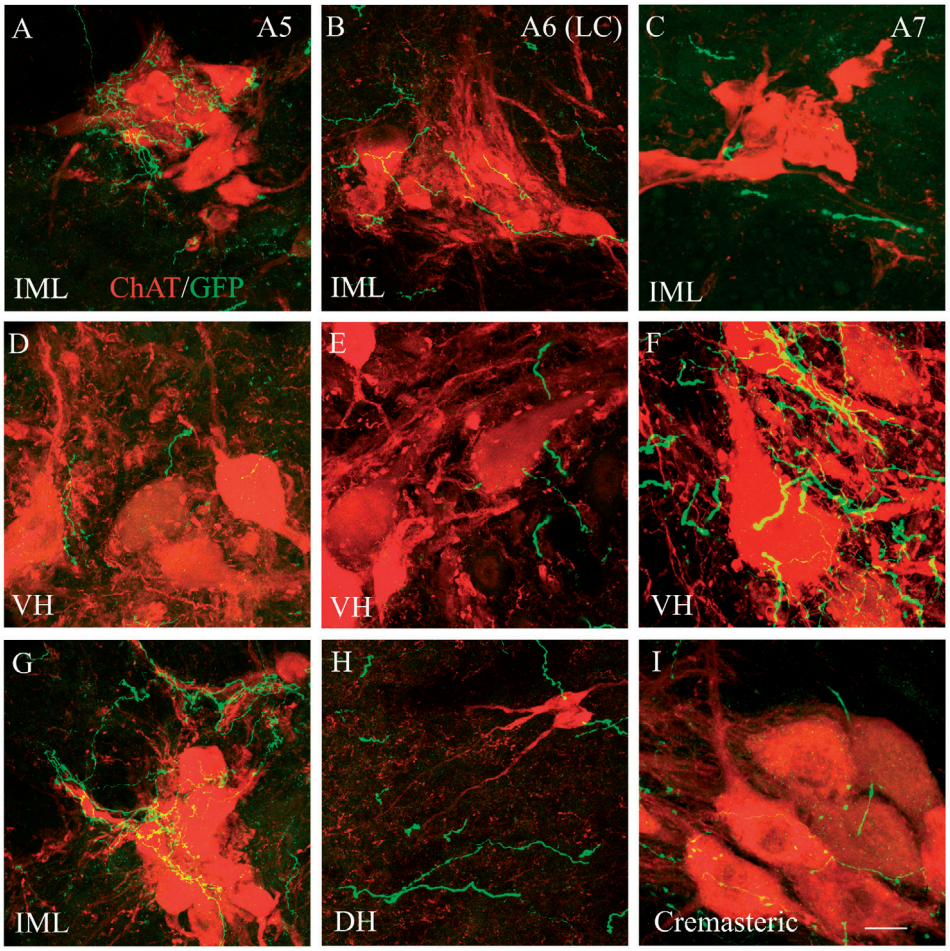

Figure 8. A series of confocal z-stack projections of sections through the spinal cord stained magenta for ChAT and green for GFP. A, D, and G show sections after an A5 injection; B, E, H after an LC (A6) injection; and C, F, I after an A7 injection. The upper row (A-C) demonstrate the extent of innervation of the IML after injections in each cell group. There is much more extensive, fine branching axonal arborization in the IML after the A5 injection. On single 1 µm sections (see fig. 9), they form boutons that are in close proximity to the dendrites and, to a lesser extent, cell bodies of IML neurons. LC and A7 axons travel in proximity to the IML, and form occasional boutons, but they do not show as much arborization in the IML. The second row (D-F) shows the innervation of the ventral horn (VH) after these injections. Large amounts of fine axonal arborization and boutons in proximity to ventral horn neurons were seen only after A7 injections. G shows another section through the IML after an A5 injection, in which the innervation is clearly related to proximal dendrites rather than cell bodies. H shows LC axons in relation to two small cholinergic interneurons in the dorsal horn (DH). The LC axons are in close proximity, but do not arborize and have few boutons in proximity to these cells. I shows A7 axons arborizing and forming boutons among cremasteric motor neurons at the L1 level of the spinal cord. This cell group was innervated by both A5 and A7 axons, but neither innervated the cremasteric neurons as intensively as their primary targets. Scale bar in I = 20 µm.

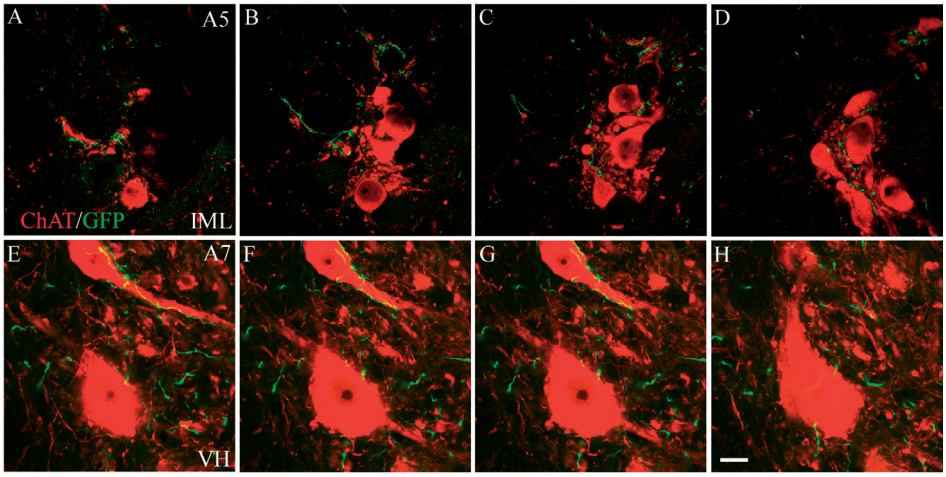

Figure 9. A series of non-consecutive 1 µm thick confocal sections through the IML after an A5 injection (A-D) and through the ventral horn after an A7 injection (E-H). These were part of the same z-stacks shown in fig. 8G and F, respectively. The thin focal planes show that the individual noradrenergic axons coursed along the surface of cholinergic cell bodies and dendrites, giving off numerous boutons. Scale bar = 20 µm.

adjacent to the dorsal columns (Figure 7B, C). However, these axons seemed to bear little relationship to the few cholinergic interneurons in the dorsal horn (Figure 8H). Labeled varicose axons were less dense in the ventral (Figure 8E) and intermediolateral (Figure 8B) horns, and generally ramified with little relationship to the cholinergic neurons, but where they encountered cholinergic neurons in either site, occasional boutons in proximity to cholinergic cell bodies or dendrites were observed.

In contrast, after injections into the A7 cell group, varicose anterogradely labeled axons tended to ramify and give off numerous boutons along the surface of the cell bodies and proximal dendrites of ventral horn cholinergic motor neurons (Figure 7D-F, G-I, 8F,I, 9E-H). There was less dense innervation of the cremasteric motor neurons, which form a characteristic cluster in the dorsal midportion of the ventral horn, at the L1-2 level (Figure 8I). The cremasteric motor neurons, like those that form Onuf's nucleus in the sacral spinal cord, express the p75 nerve growth factor receptor (24) and are important for genitourinary function. A few labeled axons were found in the remainder of the spinal cord, including the thoracic IML (Fig. 8C) and the ventral commissural nucleus, and in these locations they also gave off smaller numbers of labeled boutons along the dendrites and cell bodies of cholinergic sympathetic preganglionic neurons.

Following A5 injections, there were relatively few labeled axons along cholinergic neurons in the ventral horn (Figure 8D), but intense ramifications and numerous boutons were seen along the cell bodies and proximal dendrites of cholinergic sympathetic preganglionic neurons in the thoracic IML (Figures 7J-L, 8A,G, 9A-D). The intensity of the labeling and its density among the cholinergic neurons were best seen in the confocal z-stacks, but the relationships

of the elements within the IML were best visualized in single 1 μm thick confocal images (Figure 9A-D), in which the individual axons could be appreciated coursing along the surface of cholinergic cell bodies and dendrites and giving off numerous boutons in close apposition.

One interesting exception to the general lack of A5 axons in the ventral horn was the cremasteric motor neurons, which received innervation from both the A5 and the A7 cell group.

DISCUSSION

This study used a genetically-driven tracer to describe the noradrenergic pontine projections to the spinal cord. The details of the pontine noradrenergic innervation of the spinal cord have remained controversial, as the differences in reported data may have reflected the lack of specificity and sensitivity of conventional anterograde tracers for identifying the entire range of small, fine noradrenergic axons originating from the pons. In this study we used an AAV vector with a promoter that drives gene expression of GFP at a high level in neurons containing the Phox2 family of transcription factors, which include the pontine noradrenergic neurons. After injection of the AAV vector in the A5, LC and A7 groups, transfected neurons were detected in the injection site using an immunohistochemical procedure to label GFP. Extensive descending projections to the spinal cord were identified with GFP-immunoreactivity and virtually all of these axons also were DBH-ir. Thus for the purpose of this study, we believe that this method provided a high resolution and complete view of the descending projections from the A5, LC, and A7 cell groups to the spinal cord in Sprague-Dawley rats.

Our results indicate that the spinal projections from the A5, LC, and A7 noradrenergic cell groups are highly complementary. The LC projected mainly through the ventral funiculus and the superficial white matter of the dorsal horn, and innervated most heavily the dorsal horn. A7 descending axons were found mainly in the ventral funiculus bilaterally and projected mainly to motoneuron groups in the ventral horn. Following injections into the A5 group, descending axons travelled mainly through the ipsilateral lateral funiculus. The densest innervation from A5 was found among the thoracic sympathetic preganglionic neurons.

The advantage of this method for tracing noradrenergic neuronal projections is that it allows tracing of descending noradrenergic projections without including spinal projections from neighboring cell groups or labeling fibers of passage that may be in close proximity to the noradrenergic cell groups. Additionally, because the neurons produce the GFP continually and transport it to their most distal terminals, it is possible to visualize the entirety of the labeled neurons from their cell bodies to their most distal spinal terminals at high resolution.

Technical considerations

One unexpected technical problem in our experiments was that after injection of the AAV, a few small cells that were GFP-ir but not DBH-ir were observed at the injection sites. These small cells were NeuN-ir and therefore neurons and not glial cells. This finding is similar to that reported by Card *et al.* (12) who (using a lentiviral vector with GFP under the PRSx8

promoter) also found that not all neurons in the ventrolateral medulla that were labeled with GFP were DBH-ir. This expression in non-noradrenergic neurons most likely reflects the fact that Phox2 transcription factors are also present in some non-noradrenergic cell groups. These include cholinergic neurons in the vestibular efferent nucleus, the facial nucleus, the nucleus ambiguous, and the motoneurons of the dorsal motor nucleus of the vagus, as well as some neurons that are neither cholinergic nor noradrenergic near the A5 and A7 cell groups (11). Labeling of other small, non-noradrenergic neurons near the LC may be due to leakage of the promoter in neurons with a high multiplicity of infection in the center of the injection site, or possibly may occur because the AAV 2 inverted terminal repeats (ITR) have transactivation/promoter activity in the CNS (25). As we found that the PRSx8 promoter can clearly drive GFP expression in cells that do not make DBH, it is not really accurate to call it a "synthetic DBH" promoter. Therefore, when it is used to drive axonal labeling in noradrenergic neurons it is necessary to use careful control experiments to exclude labeling of axons from other non-noradrenergic sources.

We took such precautions in our study. We found that the small, round non-DBH-ir neurons that were labeled at the injection sites displayed a different morphology not only from the DBH-ir neurons but also from other spinally projecting cell groups in the region. These neurons also were located outside the boundaries of other cell groups that project to the spinal cord (1). In the LC region, spinally projecting neurons are located rostromedially in Barrington's nucleus, rostroventrally in the sublaterodorsal nucleus, and caudolaterally in the vestibular nuclei and fastigial nucleus (26-30). Our injection sites in the LC were confined to the LC and the underlying subcoeruleus region, and the spinally projecting cells in those regions are noradrenergic (1). Although the injection sites were very close to Barrington's nucleus (e.g., Figure 1), none of the labeled neurons were found in that nucleus, which apparently did not have the Phox2 transcription factors necessary to drive expression of GFP, and the dense projection to the sacral IML, which is characteristic of neurons in Barrington's nucleus, was not seen in our LC injections. With respect to A7 region injections, non-noradrenergic spinally-projecting neurons are located medially in the pontine reticular formation and laterally in the Kölliker-Fuse nucleus within the parabrachial complex. However, our injections were small and did not involve neurons in these other spinally projecting regions. In the A5 region, the only other spinally projecting neurons are located more dorsally in the lateral pontine reticular formation. Our injections were located ventrally and, therefore, did not involve this group. Finally, we double-labeled the spinal cord sections for GFP and DBH, and found that all GFP-ir projections were also DBH-ir, although in some cases only a faint DBH-ir signal was observed that required confocal microscopy to confirm (Figure 2). These observations indicate that it would have been difficult to map these projections in detail without the presence of the GFP label. Thus, although the PRSx8 promoter is not entirely specific in driving GFP expression exclusively in noradrenergic neurons, it does limit the involvement of nearby cell groups that do not express Phox2 transcription factors, and this viral vector construct demonstrates anterogradely labeled noradrenergic axons from the pons to the spinal cord with great fidelity and clarity. In general, the interpretation of results from neuroanatomical studies using genetically-

modified viral tracers requires caution because the expression of the tracer might not be always completely eutopic with the original gene. Nevertheless, the results can be valuable when interpreted carefully and conservatively, and when adequate controls have been done, as is the case here.

Comparison with earlier studies

Our results concerning projections of the LC are very similar to those reported by Fritschy and Grzanna (2,31) in Harlan Sprague-Dawley rats, except that they did not identify the descending pathway in the ventral funiculus, nor did they report the (relatively modest) innervation of the ventral horn that we found. On the other hand, Clark and Proudfit reported in Sasco Sprague-Dawley rats a projection from the LC through the ipsilateral ventral funiculus similar to what we observed, but described dense innervation primarily in the ventral horn of the spinal cord, with very little input to the intermediate gray matter or the dorsal horn. However, their injection sites were located quite caudally, and nearby vestibulospinal and fastigiospinal neurons that have very similar projections to the ventral horn (26; 28,29). They reported that up to 80% of the anterogradely labeled axons were DBH-ir in these experiments, but the presence of a substantial contingent of non-noradrenergic axons may have complicated the interpretation of the results.

Clark and Proudfit (32) later replicated the results of Fritschy and Grzanna using Harlan Sprague-Dawley rats and attributed the disparity in their initial findings to the difference in the source (vendor) of rats used (Harlan vs. Sasco). Recently, Howorth and colleagues (13) used a different strain of rats (Wistar) to inject a retrograde viral tracer into the dorsal horn of the spinal cord. Their viral vector contained the gene for GFP under the same PRSx8 promoter used in our study, and the authors demonstrated that 80% of the retrogradely labeled (noradrenergic) neurons were located in the LC. Thus the pattern of innervation presented here, with LC providing the dominant noradrenergic input to the dorsal horn, is likely to be the case for most, if not all, strains of rats.

The pattern of innervation of the thoracic IML that we observed seems to be consistent with previous results from studies using the transneuronal retrograde tracer Pseudorabies virus (PRV). After injection of PRV into sympathetically-innervated targets, neurons in the A5 cell group are consistently infected along with a subpopulation of neurons located in the ventral part of the LC and dorsal SubC that were consistently infected at early survival times, suggesting a direct projection to sympathetic preganglionic neurons located in the IML (33-37). However, there was a slight delay in the progression of infection in these LC neurons with respect to infection in the A5 group, which is the first and most heavily infected group at earlier survival times. This slight delay in infection might have been caused by a less dense input to the IML from the LC, as observed in the present study, or it may have indicated that the infection was transferred through additional interneuronal links at a brainstem or spinal level. The density of innervation in retrograde viral studies is an important factor in determining the multiplicity of infection, which in turn determines the time at which the viral markers can be detected. Therefore, the small number of labeled boutons observed in the thoracic IML after LC injections in the present study may explain the infection of a subpopulation of LC neurons later than the A5 group in PRV studies.

Our observations on the A7 spinal projection likewise disagree with the work of Clark and Proudfit (19) in the Sasco Sprague-Dawley rats. They reported that A7 axons mainly project through the dorsolateral funiculus and innervate the dorsal horn; this would make the projection complementary to the LC projection in that strain. However, in Harlan Sprague-Dawley rats, we found that the A7 projection runs through the ventral funiculus bilaterally, and innervates mainly the ventral horn, complementary to the LC projection in our study and others (2,13). The A7 terminals tend to be closely related to the cholinergic motor neurons in the ventral horn, with numerous appositions. Establishing the presence of synaptic contacts would require electron microscopy. However, previous studies have established that only a small minority of noradrenergic boutons in the CNS make classic synaptic contacts (38,39). Despite this lack of conventional synapses, the target cells may have noradrenergic receptors through which they respond to stimulation of the noradrenergic inputs. Hence the absence of post-synaptic specializations, which is the rule for noradrenergic axons, would not preclude a likely functional role for these profuse boutons.

Our findings on the A5 projection are consistent with the early reports by Loewy and colleagues (40) that this group provides the major noradrenergic input to the sympathetic preganglionic cell column in the thoracic spinal cord. This projection includes not only the region occupied by the IML, but the sympathetic preganglionic neurons located in the central gray matter including the dorsal commissure (central autonomic nucleus), and the clusters of preganglionic neurons that extend between these sites (intercalated nucleus). Because the A5 group has a long rostro-caudal extent, our small injections typically covered only a limited portion of the cell group. As a result, the anterograde labeling from the A5 group (other than in the sympathetic preganglionic column) appears meager in individual sections, although it does provide additional less intense inputs to the dorsal and ventral horns and to the sacral IML. Hence our results are consistent with retrograde transport studies (1) which indicate that the A5 cell group has as many spinally projecting neurons as the A7 group.

Conclusion

The novel viral tracer we have generated and employed in this study identifies a set of complementary pathways from the pontine noradrenergic cell groups to the spinal cord. This viral tracer can potentially be used in other strains and species to determine the contribution of different noradrenergic cell groups to the innervation of specific targets. However, because it is not entirely specific for expression of GFP only in noradrenergic neurons, its use must be coupled with careful controls to insure that the projections being traced are noradrenergic. By employing such controls, we have used this tracer to identify several novel axonal pathways to the spinal cord from pontine noradrenergic groups, which suggests that this tracer is more sensitive for labeling axons of passage than the anterograde tracer PHA-L used in previous studies.

The complementary pattern of the three different ponto-spinal noradrenergic pathways suggests that they play complementary roles in spinal functions. The LC, which mainly innervates the dorsal horn, has been linked with anti-nociception in Harlan Sprague-Dawley and Wistar rats (13,41). The main projection of the A7 group to motoneuron groups in our

experiments is consistent with a recent report of A7 neurons showing transneuronal labeling after injection of PRV into the thyroarytenoid muscle, which is a striated muscle innervated by motor neurons in the nucleus ambiguus complex in rats (42). The demonstration that A5 neurons project most densely to the IML where they ramify and display numerous boutons along the cell bodies and proximal dendrites of cholinergic preganglionic neurons, supports the earlier anatomical (35,36,40,43,44) and physiological (45,46) studies indicating a role in regulating sympathetic function. However, further study is needed to understand the role of these noradrenergic inputs in each of these functional contexts.

ACKNOWLEDGEMENTS

The plasmid containing PRSx8 was kindly provided by Dr. Kwang-Soo Kim from McLean Hospital, Harvard Medical School, Boston (MA). The authors thank Quan Ha for her excellent technical assistance, and Joop van Heerikhuizen and Joris Coppens from the Netherlands Institute for Neuroscience for imaging/graphics expertise. This work was supported by USPHS grants NS33987, NS072337, and HL095491.

REFERENCES

1. Westlund KN, Bowker RM, Ziegler MG, Coulter JD. 1983. Noradrenergic projections to the spinal cord of the rat. Brain Res 263(1):15-31.
2. Fritschy JM, Grzanna R. 1990. Demonstration of two separate descending noradrenergic pathways to the rat spinal cord: evidence for an intragriseal trajectory of *locus coeruleus* axons in the superficial layers of the dorsal horn. J Comp Neurol 291(4):553-82.
3. Westlund KN, Bowker RM, Ziegler MG, Coulter JD. 1981. Origins of spinal noradrenergic pathways demonstrated by retrograde transport of antibody to dopamine-beta-hydroxylase. Neurosci Lett 25(3):243-9.
4. Fritschy JM, Lyons WE, Mullen CA, Kosofsky BE, Molliver ME, Grzanna R. 1987. Distribution of *locus coeruleus* axons in the rat spinal cord: a combined anterograde transport and immunohistochemical study. Brain Res 437(1):176-80.
5. Fritschy JM, Grzanna R. 1989. Immunohistochemical analysis of the neurotoxic effects of DSP-4 identifies two populations of noradrenergic axon terminals. Neuroscience 30(1):181-97.
6. Clark FM, Proudfit HK. 1991a. The projection of *locus coeruleus* neurons to the spinal cord in the rat determined by anterograde tracing combined with immunocytochemistry. Brain Res 538(2):231-45.
7. Clark FM, Yeomans DC, Proudfit HK. 1991b. The noradrenergic innervation of the spinal cord: differences between two substrains of Sprague-Dawley rats determined using retrograde tracers combined with immunocytochemistry. Neurosci Lett 125(2):155-8.
8. Morin X, Cremer H, Hirsch MR, Kapur RP, Goridis C, Brunet JF. 1997. Defects in sensory and autonomic ganglia and absence of *locus coeruleus* in mice deficient for the homeobox gene Phox2a. Neuron 18(3):411-23.
9. Pattyn A, Goridis C, Brunet JF. 2000. Specification of the central noradrenergic phenotype by the homeobox gene Phox2b. Mol Cell Neurosci 15(3):235-43.
10. Seo H, Hong SJ, Guo S, Kim HS, Kim CH, Hwang DY, Isacson O, Rosenthal A, Kim KS. 2002. A direct role of the homeodomain proteins Phox2a/2b in noradrenaline neurotransmitter identity determination. J Neurochem 80(5):905-16.
11. Tiveron MC, Hirsch MR, Brunet JF. 1996. The expression pattern of the transcription factor Phox2 delineates synaptic pathways of the autonomic nervous system. J Neurosci 16(23):7649-60.
12. Card JP, Sved JC, Craig B, Raizada M, Vazquez J, Sved AF. 2006. Efferent projections of rat rostroventrolateral medulla C1 catecholamine

neurons: Implications for the central control of cardiovascular regulation. J Comp Neurol 499(5):840-59.

13. Howorth PW, Teschemacher AG, Pickering AE. 2009. Retrograde adenoviral vector targeting of nociresponsive pontospinal noradrenergic neurons in the rat in vivo. J Comp Neurol 512(2):141-57.
14. Hwang DY, Carlezon WA, Jr., Isacson O, Kim KS. 2001. A high-efficiency synthetic promoter that drives transgene expression selectively in noradrenergic neurons. Hum Gene Ther 12(14):1731-40.
15. Broekman ML, Comer LA, Hyman BT, Sena-Esteves M. 2006. Adeno-associated virus vectors serotyped with AAV8 capsid are more efficient than AAV-1 or -2 serotypes for widespread gene delivery to the neonatal mouse brain. Neuroscience 138(2):501-10.
16. Chamberlin NL, Du B, de LS, Saper CB. 1998. Recombinant adeno-associated virus vector: use for transgene expression and anterograde tract tracing in the CNS. Brain Res 793(1-2):169-75.
17. Russo D, Bombardi C, Grandis A, Furness JB, Spadari A, Bernardini C, Chiocchetti R. 2010. Sympathetic innervation of the ileocecal junction in horses. J Comp Neurol 518(19):4046-66.
18. Rinaman L. 2001. Postnatal development of catecholamine inputs to the paraventricular nucleus of the hypothalamus in rats. J Comp Neurol 438(4):411-22.
19. Clark FM, Proudfit HK. 1991c. The projection of noradrenergic neurons in the A7 catecholamine cell group to the spinal cord in the rat demonstrated by anterograde tracing combined with immunocytochemistry. Brain Res 547(2):279-88.
20. Clark FM, Proudfit HK. 1993. The projections of noradrenergic neurons in the A5 catecholamine cell group to the spinal cord in the rat: anatomical evidence that A5 neurons modulate nociception. Brain Res 616(1-2):200-10.
21. Barber RP, Phelps PE, Houser CR, Crawford GD, Salvaterra PM, Vaughn JE. 1984. The morphology and distribution of neurons containing choline acetyltransferase in the adult rat spinal cord: an immunocytochemical study. J Comp Neurol 229(3):329-46.
22. Canals JM, Checa N, Marco S, Akerud P, Michels A, Perez-Navarro E, Tolosa E, Arenas E, Alberch J. 2001. Expression of brain-derived neurotrophic factor in cortical neurons is regulated by striatal target area. J Neurosci 21(1):117-24.
23. Anderson CR, McLachlan EM, Srb-Christie O. 1989. Distribution of sympathetic preganglionic neurons and monoaminergic nerve terminals in the spinal cord of the rat. J Comp Neurol 283(2):269-84.
24. Koliatsos VE, Price DL, Clatterbuck RE. 1994. Motor neurons in Onuf's nucleus and its rat homologues express the p75 nerve growth factor receptor: sexual dimorphism and regulation by axotomy. J Comp Neurol 345(4):510-27.
25. Haberman RP, McCown TJ, Samulski RJ. 2000. Novel transcriptional regulatory signals in the adeno-associated virus terminal repeat A/D junction element. J Virol 74(18):8732-9.
26. Batton RR, III, Jayaraman A, Ruggiero D, Carpenter MB. 1977. Fastigial efferent projections in the monkey: an autoradiographic study. J Comp Neurol 174(2):281-305.
27. Lu J, Sherman D, Devor M, Saper CB. 2006. A putative flip-flop switch for control of REM sleep. Nature 441(7093):589-94.
28. Holstege G, Kuypers HG. 1982. The anatomy of brain stem pathways to the spinal cord in cat. A labeled amino acid tracing study. Prog Brain Res 57:145-75.
29. Rose PK, Wainwright K, Neuber-Hess M. 1992. Connections from the lateral vestibular nucleus to the upper cervical spinal cord of the cat: a study with the anterograde tracer PHA-L. J Comp Neurol 321(2):312-24.
30. Ding YQ, Takada M, Tokuno H, Mizuno N. 1995. Direct projections from the dorsolateral pontine tegmentum to pudendal motoneurons innervating the external urethral sphincter muscle in the rat. J Comp Neurol 357(2):318-30.
31. Lyons WE, Fritschy JM, Grzanna R. 1989. The noradrenergic neurotoxin DSP-4 eliminates the coeruleospinal projection but spares projections of the A5 and A7 groups to the ventral horn of the rat spinal cord. J Neurosci 9(5):1481-9.
32. Clark FM, Proudfit HK. 1992. Anatomical evidence for genetic differences in the innervation of the rat spinal cord by noradrenergic *locus coeruleus* neurons. Brain Res 591(1):44-53.

33. Smith JE, Jansen AS, Gilbey MP, Loewy AD. 1998. CNS cell groups projecting to sympathetic outflow of tail artery: neural circuits involved in heat loss in the rat. Brain Res 786(1-2):153-64.
34. Sly DJ, Colvill L, McKinley MJ, Oldfield BJ. 1999. Identification of neural projections from the forebrain to the kidney, using the virus pseudorabies. J Auton Nerv Syst 77(2-3):73-82.
35. Cano G, Sved AF, Rinaman L, Rabin BS, Card JP. 2001. Characterization of the central nervous system innervation of the rat spleen using viral transneuronal tracing. J Comp Neurol 439(1):1-18.
36. Cano G, Passerin AM, Schiltz JC, Card JP, Morrison SF, Sved AF. 2003. Anatomical substrates for the central control of sympathetic outflow to interscapular adipose tissue during cold exposure. J Comp Neurol 460(3):303-26.
37. Cano G, Card JP, Sved AF. 2004. Dual viral transneuronal tracing of central autonomic circuits involved in the innervation of the two kidneys in rat. J Comp Neurol 471(4):462-81.
38. Balcita-Pedicino JJ, Rinaman L. 2007. Noradrenergic axon terminals contact gastric preautonomic neurons in the paraventricular nucleus of the hypothalamus in rats. J Comp Neurol 501(4):608-18.
39. Haxhiu MA, Kc P, Neziri B, Yamamoto BK, Ferguson DG, Massari VJ. 2003. Catecholaminergic microcircuitry controlling the output of airway-related vagal preganglionic neurons. J Appl Physiol 94(5):1999-2009.
40. Loewy AD, McKellar S, Saper CB. 1979. Direct projections from the A5 catecholamine cell group to the intermediolateral cell column. Brain Res 174(2):309-14.
41. Lu J, Nelson LE, Franks N, Maze M, Chamberlin NL, Saper CB. 2008. Role of endogenous sleep-wake and analgesic systems in anesthesia. J Comp Neurol 508(4):648-62.
42. Van Daele DJ, Cassell MD. 2009. Multiple forebrain systems converge on motor neurons innervating the thyroarytenoid muscle. Neuroscience 162(2):501-24.
43. Loewy AD, Marson L, Parkinson D, Perry MA, Sawyer WB. 1986. Descending noradrenergic pathways involved in the A5 depressor response. Brain Res 386(1-2):313-24.
44. Strack AM, Sawyer WB, Hughes JH, Platt KB, Loewy AD. 1989. A general pattern of CNS innervation of the sympathetic outflow demonstrated by transneuronal pseudorabies viral infections. Brain Res 491(1):156-62.
45. Stanek KA, Neil JJ, Sawyer WB, Loewy AD. 1984. Changes in regional blood flow and cardiac output after L-glutamate stimulation of A5 cell group. Am J Physiol 246(1 Pt 2):H44-H51.
46. Huangfu DH, Koshiya N, Guyenet PG. 1991. A5 noradrenergic unit activity and sympathetic nerve discharge in rats. Am J Physiol 261(2 Pt 2):R393-R402.